International Journal of Wireless and Ad Hoc Communication

♦ ISSN: 2692-4056 Vol: 11, No. 01, 2027 ♦ PP. 01–11

Article DOI: https://doi.org/10.54216/IJWAC.110101

FULL LENGTH ARTICLE

Pareto-Based Joint Optimization of Node Activity and Communication in Dense IoT Sensor Networks

Upendra Kumar Singh[1,*] **Monika Nanda**[2]

[1] Department of Computer Science and Engineering, SRMS College of Engineering and Technology, Bareilly, Uttar Pradesh, India
[2] Department of Electronics and Communication Engineering, Birla Institute of Applied Sciences, Bhimtal, Nainital, Uttarakhand, India

Emails: 1up2804@gmail.com; 2monikananda2012@gmail.com

Received: June 25, 2026 Revised: September 14, 2026 Accepted: November 05, 2026 ⋆ Corresponding author

ABSTRACT

Dense IoT sensor networks face a fundamental trade-off between energy efficiency, communication delay, and packet delivery reliability. As network density increases, controlling node activity and communication behavior becomes increasingly important because energy-saving decisions can affect forwarding availability and communication performance. This study presents a Pareto-based framework for jointly optimizing node activity and communication decisions in dense IoT sensor networks. The proposed formulation considers total energy consumption, average end-to-end delay, and packet delivery reliability as competing objectives, with NSGA-II employed as the multi-objective optimization engine. The study evaluates three network densities comprising 50, 100, and 200 nodes. For each density, a selected Pareto configuration is independently validated using five random seeds and 1000 simulation rounds per seed. The validated configurations consume 8.6090 J, 28.1479 J, and 70.6780 J of mean energy for 50, 100, and 200 nodes, respectively, while the corresponding mean delays are 0.08458 s, 0.13441 s, and 0.19901 s. The mean PDR values are 36.4393%, 46.6317%, and 42.5616%, respectively. The results show that increasing network density leads to substantially higher energy consumption and delay, while packet delivery reliability does not improve monotonically. The findings demonstrate that joint activity and communication control provides distinct Pareto operating points and that multi-seed validation is important for assessing their stability under stochastic network conditions. The study provides a transparent density-wise analysis of the energy–delay–reliability trade-off in dense IoT sensor networks.

Keywords: Wireless Sensor Networks ▪ Internet of Things (IoT) ▪ Multi-Objective Optimization ▪ NSGA-II ▪ Duty-Cycle Control ▪ Energy-Efficient Routing ▪ Pareto Optimization

1. INTRODUCTION

The rapid deployment of Internet of Things (IoT) technologies has resulted in increasingly dense wireless sensor networks in which a large number of resource-constrained devices cooperate to sense, process, and transmit information. Such networks are widely used in environmental monitoring, smart agriculture, industrial monitoring, healthcare, and other distributed sensing applications. However, the limited energy resources of sensor nodes make energy-efficient communication a fundamental requirement for sustained network operation [1].

In a wireless sensor network, communication-related activities such as packet transmission, reception, and forwarding consume a significant portion of the available energy. The problem becomes more challenging as the number of deployed nodes increases. Dense deployments provide more

© 2027 The Author(s). Published by ASPG. This article is licensed under CC BY 4.0.

potential communication opportunities, but they can also introduce additional forwarding activity, longer communication paths, contention, and redundant network activity. Consequently, increasing node density does not necessarily lead to a proportional improvement in network reliability or energy efficiency.

One established approach to reducing energy consumption is duty-cycle control, in which nodes alternate between active and inactive states. Sleep scheduling can reduce unnecessary radio activity and consequently conserve energy. Recent research has explored adaptive and optimization-based sleep scheduling, including approaches that jointly consider sleep scheduling with routing and clustering decisions [2], as well as approaches that integrate optimized sleep/awake scheduling with adaptive routing [3]. These studies highlight the importance of controlling node activity according to network conditions rather than relying exclusively on permanently active nodes.

Routing decisions provide another important mechanism for controlling network energy consumption and communication performance. Energy-efficient routing has been studied extensively, beginning with clustering-based approaches such as LEACH [4] and extending to energy-aware ant-colony routing methods [5], opportunistic routing [6], and multi-objective clustering and routing strategies [7, 8]. Recent research has also investigated learning-based routing with attack detection and adaptive relay strategies for agricultural monitoring [9, 10]. These developments demonstrate that routing decisions directly influence the energy, delay, and reliability characteristics of resource-constrained networks.

The relationship between node activity and routing is particularly important in dense IoT networks. A routing path depends on the availability of suitable forwarding nodes, while the activity state of a node determines whether that node can participate in communication at a given time. Therefore, independently optimizing node activity and routing may overlook their interaction. A reduction in node activity can decrease energy consumption but may also reduce forwarding opportunities, whereas increased activity can improve communication availability at the cost of additional energy consumption. Recent work combining duty cycling with routing optimization further illustrates the relevance of this interaction [11].

At the same time, intelligent optimization techniques are increasingly being used to address the conflicting requirements of energy efficiency and communication performance. Recent studies have applied multi-objective optimization to clustering and routing [7, 8], while AI-driven approaches have been investigated for energy-efficient IoT routing [12] and secure routing [9]. Other recent optimization-based routing methods have employed cluster-head rotation and bio-inspired clustering and routing [13, 14, 15]. Although these approaches demonstrate the effectiveness of optimization for improving individual or multiple network objectives, the complexity of the optimization mechanism can make it difficult to isolate the effects of individual network decisions.

The energy-efficient operation of a dense IoT network is therefore naturally a multi-objective problem. Minimizing energy consumption may conflict with minimizing communication delay and maximizing packet delivery reliability. A configuration with very low node activity may consume less energy but can provide fewer communication opportunities. Conversely, maintaining higher activity or selecting more communication paths may improve delivery performance while increasing energy expenditure. Multi-objective optimization provides a way to preserve these competing solutions as a set of Pareto alternatives rather than forcing them into a single weighted objective. NSGA-II is particularly suitable for this purpose because it was designed to efficiently identify and maintain diverse non-dominated solutions in multi-objective search spaces [16].

Despite the growing body of work on energy-efficient routing, sleep scheduling, clustering, and intelligent optimization, there remains a need for a transparent experimental analysis of how joint node activity and communication decisions affect the energy–delay–reliability trade-off under increasing network density. The objective of this study is not to claim that joint optimization has never been investigated. Instead, the study focuses on a lightweight Pareto-based formulation in which node activity and communication decisions are represented jointly and their effects are examined systematically across different network densities.

Accordingly, this work investigates the following research question:

> *How does jointly controlling node activity and communication decisions affect the energy–delay–reliability trade-off of dense IoT sensor networks as network density increases?*

To address this question, the study evaluates three network densities, namely 50, 100, and 200 nodes. Total energy consumption, average end-to-end delay, and packet delivery reliability are treated as competing objectives. NSGA-II is used as the optimization engine to generate non-dominated solutions, after which selected configurations are evaluated using independent random seeds to examine the stability of the observed performance.

The main contributions of this work are:

1. A joint activity–communication formulation for dense IoT sensor networks that represents node activity and communication decisions within a common optimization framework.
2. A Pareto-based multi-objective optimization approach that simultaneously considers energy consumption, end-to-end delay, and packet delivery reliability without reducing the problem to a single weighted objective.
3. A density-wise analysis using 50-, 100-, and 200-node networks to investigate how the energy–delay–reliability trade-off changes as network density increases.
4. A multi-seed validation procedure for the selected Pareto configurations to examine the robustness of the observed results under stochastic simulation conditions.

The remainder of the paper is organized as follows. Section 2 reviews related research on energy-efficient communication, duty cycling, routing, and multi-objective optimization in WSN and IoT networks. Section 3 presents the network

model, joint decision representation, objective functions, constraints, NSGA-II optimization procedure, and validation methodology. Section 4 presents and discusses the experimental results for different network densities. Section 5 discusses the implications and limitations of the findings, and Section 6 concludes the paper and outlines directions for future work.

2. RELATED WORK

Wireless sensor networks (WSNs) are characterized by resource-constrained sensor nodes that communicate over wireless links, making energy-efficient operation an important design consideration [1]. In dense deployments, the interaction between node activity, communication, and routing becomes more significant because network performance depends not only on the availability of individual nodes but also on the forwarding paths formed among them.

One widely used approach for reducing energy consumption is sleep scheduling or duty-cycle control. The basic idea is to allow nodes to alternate between active and sleep states so that unnecessary radio activity can be reduced. However, reducing the active period may also affect connectivity and packet delivery. Recent work has therefore considered sleep scheduling together with other network decisions. Abbas et al. proposed a two-phase genetic algorithm for jointly addressing sleep scheduling, routing, and clustering in heterogeneous WSNs [2]. Roberts et al. combined optimized sleep/awake scheduling with adaptive routing, illustrating the potential of coordinating activity and communication decisions [3]. These studies indicate that activity control cannot always be considered independently of the communication structure.

Routing optimization has also been extensively investigated as a means of improving energy efficiency and network lifetime. Heinzelman et al. introduced LEACH, an energy-efficient communication protocol based on clustering and cluster-head selection [4]. More recent studies have explored optimization-based routing mechanisms. Yang et al. developed a cluster-based routing protocol combining a snake optimizer with a minimum spanning tree [14], while Tawfeek et al. proposed a modified ant-colony algorithm for energy-efficient and reliable WSN routing [5]. Other recent approaches have incorporated clustering and routing into multi-objective optimization frameworks [7, 8].

Opportunistic and adaptive routing mechanisms provide another direction for improving communication efficiency. Lata et al. proposed FCM-OR, a local density-aware opportunistic routing protocol designed for energy-efficient WSN communication [6]. Energy-efficient routing has also been studied in agricultural monitoring, including adaptive data relay for crop growth monitoring [10]. These approaches demonstrate that routing performance is influenced by the characteristics of the surrounding nodes and the communication environment.

Recent research has increasingly incorporated intelligent optimization and learning techniques into WSN routing. Kavitha et al. proposed a learning-based adaptive routing approach that addresses energy efficiency and attack detection [9]. Wang et al. proposed a Spider Wasp Optimizer-based multihop protocol that jointly optimizes cluster-head selection and inter-cluster routing [15]. A recent comprehensive review by Thakur et al. further highlights the growing use of AI-driven techniques for energy-efficient routing in IoT-based WSNs [12]. Although these approaches can provide sophisticated optimization mechanisms, their complexity may make it more difficult to isolate the contribution of individual network decisions.

Duty cycling and routing have also been considered jointly in IoT networks. Rana et al. proposed a hybrid energy-efficient routing approach combining duty cycling with an improved ant-colony method [11]. This line of work is particularly relevant to the present study because it demonstrates that node activity and communication decisions can interact and should not necessarily be optimized as completely independent mechanisms.

The use of multi-objective optimization is appropriate when energy efficiency must be considered together with other network performance requirements. Recent studies have formulated energy-efficient clustering and routing as multi-objective optimization problems [7, 8]. In such problems, reducing energy consumption can conflict with communication performance, network lifetime, or reliability. A Pareto-based formulation allows these competing objectives to be represented simultaneously rather than combining them into a single fixed weighted objective.

NSGA-II is a well-established evolutionary multi-objective optimization algorithm that uses non-dominated sorting and crowding-distance mechanisms to maintain a diverse set of Pareto-optimal solutions [16]. In the present study, NSGA-II is used as the optimization engine for exploring the joint decision space. The algorithm itself is therefore not claimed as the principal novelty of the work.

The reviewed literature shows three relevant directions: activity or sleep scheduling [2, 3], energy-efficient and optimized routing [5, 6, 9, 10, 13, 14, 15], and joint or multi-objective approaches that combine network decisions [2, 7, 8, 11]. These studies provide the foundation for investigating the interaction between node activity and communication behavior. However, the present work focuses specifically on a lightweight and transparent Pareto formulation in which node activity and communication decisions are represented jointly and evaluated against energy consumption, end-to-end delay, and packet delivery reliability across different network densities.

Rather than claiming that previous studies have not jointly considered these factors, this study positions its contribution around the controlled analysis of the energy–delay–reliability trade-off under increasing network density, together with multi-seed validation of the selected Pareto configurations. The experimental design therefore considers 50-, 100-, and 200-node networks and evaluates the selected configurations under independent random seeds to examine the consistency of their observed behavior.

3. PROBLEM FORMULATION AND METHODOLOGY

A joint optimization framework is presented for node activity and communication decisions in dense IoT sensor networks. The methodology comprises the network model, decision representation, multi-objective optimization, Pareto solution selection, and independent validation.

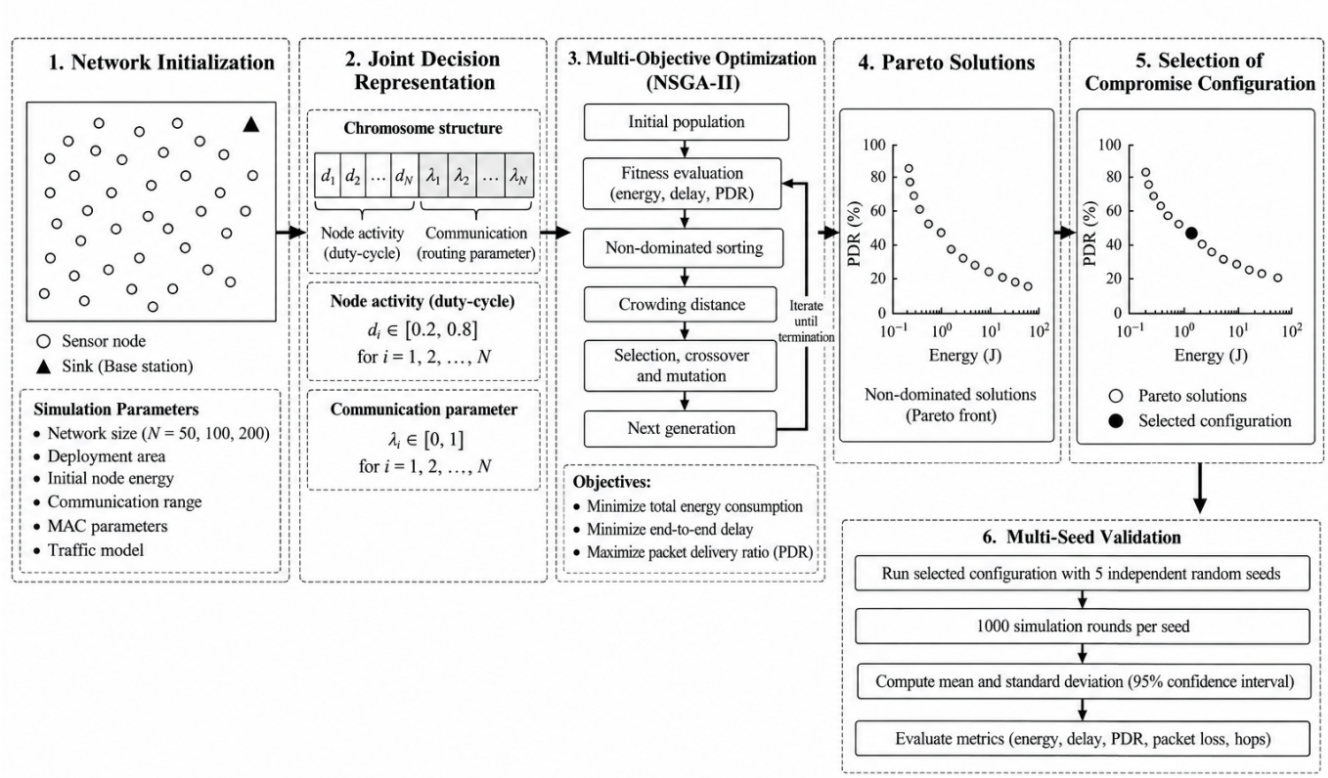


Figure 1. Proposed framework and experimental workflow for joint optimization of node activity and communication in dense IoT sensor networks.

3.1 Network Model

Consider a dense IoT sensor network consisting of N sensor nodes and one sink node. Each sensor node periodically generates data and communicates with the sink through one or more wireless forwarding nodes. The network is evaluated for different densities, represented by $N = 50$, 100, and 200 nodes.

Each node is associated with a node-activity parameter and a communication parameter. The activity parameter determines the fraction of the operating cycle during which the node remains active, whereas the communication parameter influences the routing decision. The communication range is fixed at 25 m throughout the experiments.

Let a_i denote the activity level of node i. The activity values are bounded as follows:

$$a_{\min} \leq a_i \leq a_{\max}. \tag{1}$$

The limits used in this study are

$$a_{\min} = 0.2, \qquad a_{\max} = 0.8. \tag{2}$$

Thus, the formulation permits heterogeneous node activity rather than imposing a single duty-cycle value on all nodes.

3.2 Joint Activity and Communication Representation

The proposed solution is represented by a chromosome containing the node-wise activity and communication decision variables. For node i, the activity variable is represented by a_i, while the routing parameter is represented by λ_i. The chromosome can therefore be expressed as

$$\mathbf{x} = [a_1, a_2, \ldots, a_N, \lambda_1, \lambda_2, \ldots, \lambda_N]. \tag{3}$$

This representation allows the optimizer to search for activity and communication configurations simultaneously. The resulting solution is not required to use the same activity or routing parameter for every node. The node activity values are bounded by the predefined duty-cycle limits. Communication decisions must satisfy the connectivity and routing feasibility conditions required by the network model, including communication-range and loop-free routing constraints.

3.3 Multi-Objective Optimization

The optimization problem is formulated using three competing objectives: minimization of total energy consumption, minimization of average end-to-end delay, and minimization of packet delivery loss, equivalently maximization of PDR. The energy objective is

$$\min f_1(\mathbf{x}) = E_{\text{total}}, \tag{4}$$

where E_{total} represents the total energy consumed by the network during the simulation. The delay objective is

$$\min f_2(\mathbf{x}) = D_{\text{avg}}, \tag{5}$$

where D_{avg} denotes the average end-to-end packet delay. Packet delivery ratio is defined as

$$\text{PDR} = \frac{P_{\text{delivered}}}{P_{\text{generated}}} \times 100\%. \tag{6}$$

Since the optimization procedure is expressed as minimization, the reliability objective can equivalently be represented as

$$\min f_3(\mathbf{x}) = 1 - \frac{\text{PDR}}{100}. \tag{7}$$

The three objectives are conflicting in nature. Increasing node activity or communication opportunities may improve packet delivery and reduce communication delay, but can also increase energy consumption. Conversely, reducing activity can save energy while potentially affecting forwarding availability and delivery reliability. The Pareto formulation preserves these competing solutions instead of reducing the problem to a single weighted objective.

3.4 Constraints

The candidate solutions are required to satisfy the operational constraints of the network.

Duty-cycle constraint

$$0.2 \leq a_i \leq 0.8, \qquad i = 1, \ldots, N. \tag{8}$$

Communication-range constraint A communication link between nodes i and j is feasible only when their separation does not exceed the specified communication range:

$$d_{ij} \leq R_c, \qquad R_c = 25 \text{ m}. \tag{9}$$

Connectivity constraint Every source node must have a feasible communication path to the sink. A candidate solution that cannot provide sink connectivity is treated as infeasible.

Loop-free routing constraint The selected forwarding relationships must not create routing loops. A packet must therefore progress through a valid forwarding sequence toward the sink. These constraints ensure that the optimization does not favor numerically attractive but operationally invalid configurations.

3.5 NSGA-II Optimization

The Non-dominated Sorting Genetic Algorithm II (NSGA-II) is employed as the multi-objective optimization engine [16]. For each network size, an initial population of candidate chromosomes is generated and evaluated using the three objective functions. NSGA-II ranks candidate solutions according to Pareto dominance and uses crowding distance to maintain diversity among non-dominated solutions [16]. Through successive generations, the population is evolved using the corresponding selection, crossover, and mutation operations.

The output of this stage is a Pareto set containing solutions that represent different compromises among energy consumption, delay, and packet delivery reliability. NSGA-II is used here as the search mechanism; the methodological focus of the study is the joint representation of node activity and communication decisions and the subsequent density-wise and robustness analysis.

3.6 Pareto Solution Selection

The final NSGA-II population contains multiple non-dominated solutions. Since no single solution necessarily minimizes all three objectives simultaneously, one compromise solution is selected from the final Pareto set for subsequent validation. The selected solution represents a balanced operating point rather than the independently best solution for energy, delay, or reliability. The same selection procedure is applied to each network size to maintain consistency across the density-wise experiments.

The selected chromosomes are subsequently subjected to independent stochastic validation. This separation ensures that the optimization stage and validation stage serve different purposes: NSGA-II identifies candidate trade-offs, while multi-seed simulation evaluates the stability of the selected configuration.

3.7 Robust Multi-Seed Validation

To assess the sensitivity of the selected configurations to stochastic simulation conditions, each selected chromosome is evaluated using five independent random seeds:

$$\mathscr{S} = \{42, 123, 2024, 3407, 7777\}. \tag{10}$$

Each seed is evaluated for 1000 simulation rounds using the same communication range and network configuration. Thus, three selected configurations and five seeds result in a total of 15 validation simulations.

For each network size, the validation procedure records total energy, average delay, PDR, packet loss, and average hop count. The mean and standard deviation are calculated across the five seeds. A 95% confidence interval is also calculated for the reported metrics. This procedure provides an estimate of both the average performance and the variability of the selected Pareto configuration across independent stochastic realizations. For a metric x observed over the five independent seeds, the sample mean is

$$\bar{x} = \frac{1}{5} \sum_{k=1}^{5} x_k. \tag{11}$$

The sample standard deviation is used to quantify variation across seeds, and the 95% confidence interval is derived from the five observations.

3.8 Evaluation Metrics

The principal evaluation metrics are defined as follows:

- **Energy consumption:** total energy consumed by all participating nodes during the simulation, measured in joules.
- **Average delay:** mean end-to-end delay of successfully delivered packets, measured in seconds.
- **Packet Delivery Ratio (PDR):**

$$\text{PDR} = \frac{P_{\text{delivered}}}{P_{\text{generated}}} \times 100\%.$$

- **Packet loss:** Packet Loss $= 100 - \text{PDR}$.
- **Average hops:** mean number of forwarding hops associated with packet delivery.
- **Duty cycle:** node activity level used to determine the active fraction of the operating cycle.
- **Routing parameter λ:** node-level routing parameter incorporated into the communication decision representation.

3.9 Experimental Configuration

The experiments use three network sizes:

$$N \in \{50, 100, 200\}. \tag{12}$$

The communication range is fixed at 25 m, and each validation run consists of 1000 simulation rounds. The same five random seeds are used for all three network sizes.

For the final validation, the selected Trial-4.3 configurations are listed below. The node-wise duty-cycle and routing-λ values contained in these selected chromosomes are retained during validation rather than replacing them with newly generated values. This preserves the correspondence between the optimized solution and its independent validation.

Selected Trial-4.3 candidates for final validation

Network Size	Selected Candidate
50	24
100	17
200	1

The complete experimental workflow is summarized as network initialization, chromosome evaluation, NSGA-II optimization, Pareto-set formation, compromise selection, five-seed validation, and statistical analysis. The resulting validated measurements form the basis of the results and discussion presented in the following section.

4. RESULTS AND DISCUSSION

The experimental results are based on the selected Pareto configurations for 50, 100, and 200 nodes. Each configuration was independently evaluated using five random seeds and 1000 simulation rounds per seed. The reported values therefore represent the mean behavior of the selected configurations across the five stochastic realizations.

4.1 Density-Wise Performance

Table 1 presents the validated performance of the selected configurations.

The results show a clear increase in mean energy consumption as the network size increases. Energy rises from 8.6090 J for 50 nodes to 28.1479 J for 100 nodes and 70.6780 J for 200 nodes. The increase indicates that larger network instances require substantially greater energy expenditure under their respective selected configurations. Figure 2 illustrates the corresponding validated energy consumption and its variation across the five independent seeds.

Average delay follows a similar trend. The delay increases from 0.08458 s at 50 nodes to 0.13441 s at 100 nodes and 0.19901 s at 200 nodes. Average hop count also increases from 3.7421 to 5.4177 and 7.2395, respectively. The simultaneous increase in hop count and delay suggests that the communication paths in the larger network instances involve more forwarding steps.

PDR does not follow the same monotonic pattern. It increases from 36.4393% for 50 nodes to 46.6317% for 100 nodes and then decreases to 42.5616% for 200 nodes. Thus, the present results do not indicate a simple relationship in which increasing node density continuously improves packet delivery. Instead, the reliability response varies with the selected configuration and network size.

The packet-loss values are the complementary measure of PDR, decreasing from 63.5607% for 50 nodes to 53.3683% for 100 nodes and then increasing to 57.4384% for 200 nodes. This behavior is consistent with the corresponding PDR values.

4.2 Behavior of Joint Decision Variables

Table 2 reports the aggregate activity and routing characteristics of the validated chromosomes.

The mean duty-cycle values remain close to 0.5 for all three network sizes. At the same time, the minimum and maximum values reach the predefined bounds of 0.2 and 0.8. This confirms that the selected chromosomes contain heterogeneous node-activity levels rather than a single common activity value.

The mean routing-λ values are 0.469351, 0.541676, and 0.509138 for 50, 100, and 200 nodes, respectively. No monotonic increase or decrease is observed. This indicates that the communication parameter changes according to the selected Pareto configuration rather than being directly determined by network size.

The combination of heterogeneous duty-cycle values and routing parameters is consistent with the joint decision formulation. The optimization does not select node activity independently of communication behavior; both components are retained in the chromosome and evaluated together. The node-level duty-cycle and routing-parameter profiles of the selected chromosomes are presented in Figure 3.

4.3 Robustness of the Selected Configurations

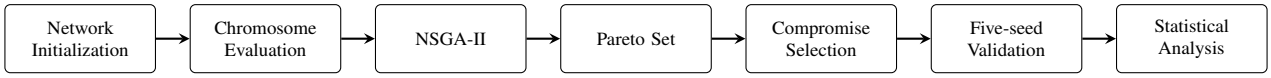
The five-seed validation provides information about the variability of the selected configurations. For energy consumption, the standard deviation increases from 0.4275 J for 50 nodes to 2.1288 J for 200 nodes. However, the relative variation remains considerably smaller than the corresponding increase in the mean energy.

The delay standard deviations are 0.00347 s, 0.00737 s, and 0.00851 s for 50, 100, and 200 nodes, respectively. The PDR standard deviations are 6.8676, 3.2558, and 1.8428 percentage points. The corresponding 95% confidence intervals are presented in Table 3.

The relatively larger PDR variation for the 50-node case indicates greater sensitivity to the stochastic realization in this configuration. For the larger networks, the PDR variation across the five seeds is lower. These confidence intervals should be interpreted as estimates of variability across the five validation seeds and not as evidence of statistical superiority over another protocol.

4.4 Energy–Delay–Reliability Trade-Off

The results demonstrate the trade-off that motivated the Pareto formulation. The selected configurations do not simultaneously provide the minimum energy, minimum delay, and maximum PDR. Instead, each represents a compromise among the competing objectives. The complete NSGA-II Pareto solutions for the considered network densities are shown in



Experimental workflow

Table 1. Performance of selected configurations under multi-seed validation

Nodes	Candidate	Energy (J)	Delay (s)	PDR (%)	Packet Loss (%)	Average Hops
50	24	8.6090 ± 0.4275	0.08458 ± 0.00347	36.4393 ± 6.8676	63.5607 ± 6.8676	3.7421 ± 0.1465
100	17	28.1479 ± 1.0215	0.13441 ± 0.00737	46.6317 ± 3.2558	53.3683 ± 3.2558	5.4177 ± 0.1553
200	1	70.6780 ± 2.1288	0.19901 ± 0.00851	42.5616 ± 1.8428	57.4384 ± 1.8428	7.2395 ± 0.1279

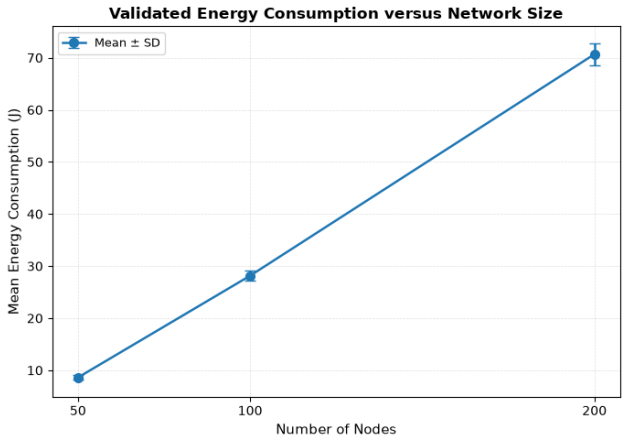


Figure 2. Validated mean energy consumption with standard deviation across different network sizes.

Table 2. Activity and communication characteristics of selected chromosomes

Nodes	Candidate	Mean Duty Cycle	Min Duty Cycle	Max Duty Cycle	Mean Routing λ
50	24	0.50855	0.2	0.8	0.469351
100	17	0.51374	0.2	0.8	0.541676
200	1	0.483275	0.2	0.8	0.509138

Figure 4, where the energy–delay relationship is presented with PDR represented by the color scale.

The 50-node configuration has the lowest energy and delay among the three evaluated configurations, but it also has the lowest mean PDR. The 100-node configuration provides the highest mean PDR of the three cases, while requiring higher energy and delay than the 50-node configuration. At 200 nodes, energy and delay increase further, whereas PDR falls relative to the 100-node case.

This behavior illustrates why a single performance metric would provide an incomplete description of the optimized network. The Pareto-based formulation retains the conflicting objectives and enables a compromise solution to be selected according to the intended operating requirements.

4.5 Density Scaling

A particularly important outcome is the change in system behavior with network density. Increasing the network size from 50 to 200 nodes results in approximately 8.2 times the mean energy consumption and approximately 2.35 times the mean delay. Average hops increase by approximately 93.5% over the same range. Figure 5 presents the corresponding validated delay and hop-count behavior across the three network

Table 3. 95% confidence intervals of validated performance measures

Nodes	Energy CI95 ($\pm$ J)	Delay CI95 ($\pm$ s)	PDR CI95 ($\pm$ percentage points)
50	0.5307	0.00431	8.5259
100	1.2681	0.00915	4.0419
200	2.6428	0.01056	2.2878

sizes.

However, PDR changes from 36.4393% to 42.5616%, with its maximum occurring at 100 nodes. The corresponding PDR and packet-loss behavior is illustrated in Figure 6. Therefore, the scaling results suggest that increasing node density introduces additional communication cost without guaranteeing a proportional improvement in delivery reliability.

These observations provide the basis for evaluating the central research question: how joint control of node activity and communication decisions affects the energy–delay–reliability trade-off as network density increases. The answer from the present experiments is not a single uniformly improving trend; rather, the trade-off shifts with network size, and the selected Pareto configuration provides a different balance at each density.

5. DISCUSSION

The experimental results indicate that joint optimization of node activity and communication decisions produces different operating points as network density changes. The observed behavior is particularly relevant because energy consumption, delay, and packet delivery reliability do not improve simultaneously with increasing network size.

5.1 Effect of Network Density

The increase in network size from 50 to 200 nodes is accompanied by a substantial increase in energy consumption and communication delay. Mean energy increases from 8.6090 J for 50 nodes to 28.1479 J for 100 nodes and 70.6780 J for 200 nodes. Average delay similarly increases from 0.08458 s to 0.13441 s and 0.19901 s.

One factor reflected in these results is the increase in average hop count. The mean hop count changes from 3.7421 for 50 nodes to 5.4177 for 100 nodes and 7.2395 for 200 nodes. More forwarding stages provide a direct mechanism through which communication activity and delay can increase in larger network instances.

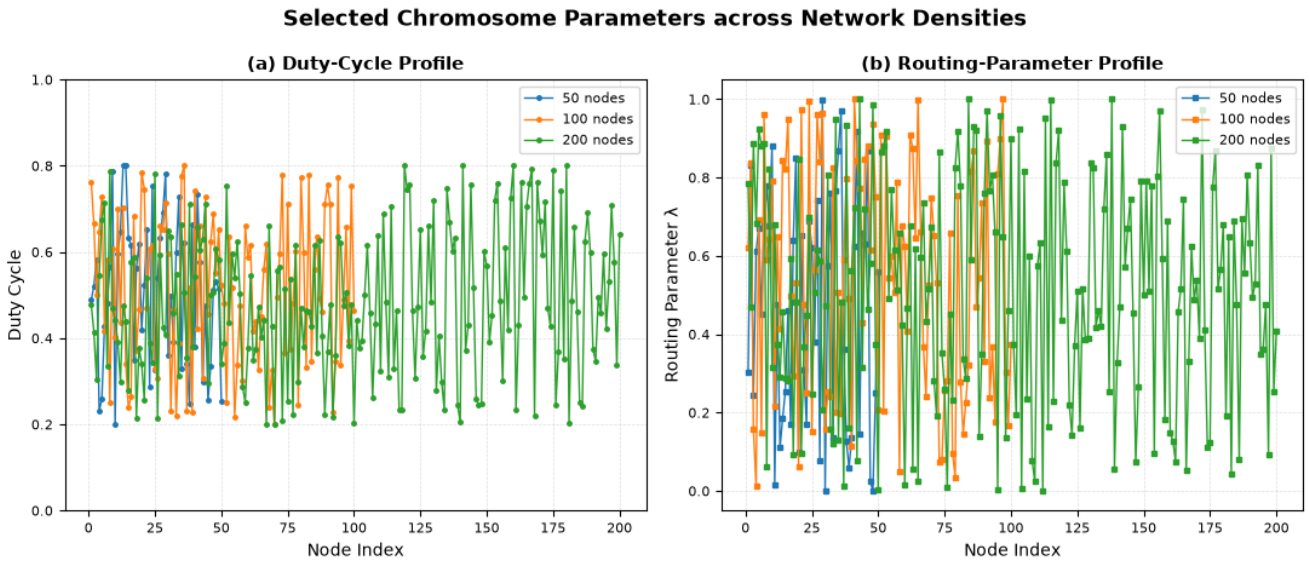


Figure 3. Node-level duty-cycle and routing-parameter profiles of the selected configurations across different network densities: (a) duty-cycle profile and (b) routing-parameter λ profile.

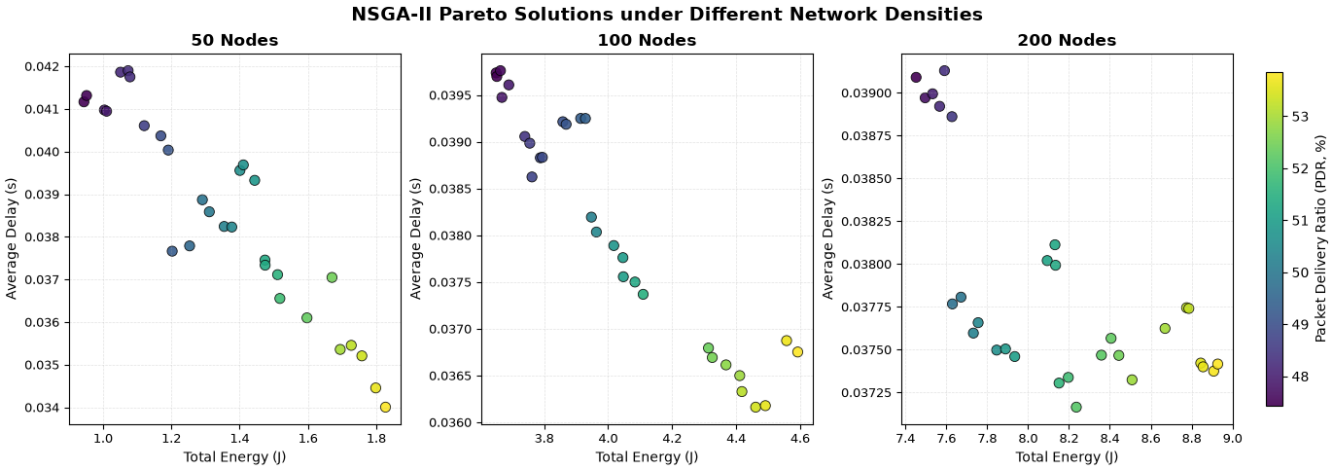


Figure 4. NSGA-II Pareto solutions for different network densities, showing the energy–delay trade-off with packet delivery ratio represented by the color scale.

The relationship between density and reliability is less straightforward. PDR increases from 36.4393% at 50 nodes to 46.6317% at 100 nodes, but decreases to 42.5616% at 200 nodes. Hence, higher node density does not automatically translate into higher delivery reliability. The selected activity and communication configuration, together with the resulting forwarding structure, affects the final reliability.

5.2 Joint Activity and Communication Decisions

The selected chromosomes exhibit heterogeneous duty-cycle values between 0.2 and 0.8, with mean values close to 0.5 for all three network sizes. This is important because a homogeneous activity policy would assign the same activity level to every node, whereas the present formulation permits different nodes to operate at different activity levels.

The routing-λ values also vary across the selected configurations. Their mean values are 0.469351, 0.541676, and 0.509138 for 50, 100, and 200 nodes, respectively. The absence of a monotonic pattern suggests that the communication parameter is selected as part of the overall Pareto trade-off rather than being determined solely by network density.

The results therefore support analyzing node activity and communication behavior as coupled decisions. Changing the activity state of a node can affect its availability as a forwarding node, while changing communication decisions can alter the number and characteristics of active forwarding paths. Their combined effect is reflected in the resulting energy, delay, and PDR.

5.3 Energy–Delay–Reliability Trade-Off

The three evaluated configurations demonstrate different compromises among the optimization objectives. The 50-node configuration achieves the lowest mean energy and delay, but its mean PDR is also the lowest. The 100-node configuration provides the highest PDR among the three selected configurations, while requiring more energy and producing greater delay. The 200-node configuration incurs the highest energy and delay, while its PDR remains below that of the 100-node case.

This behavior is consistent with the multi-objective nature of the problem. Energy-efficient operation cannot be interpreted independently of communication reliability and de-

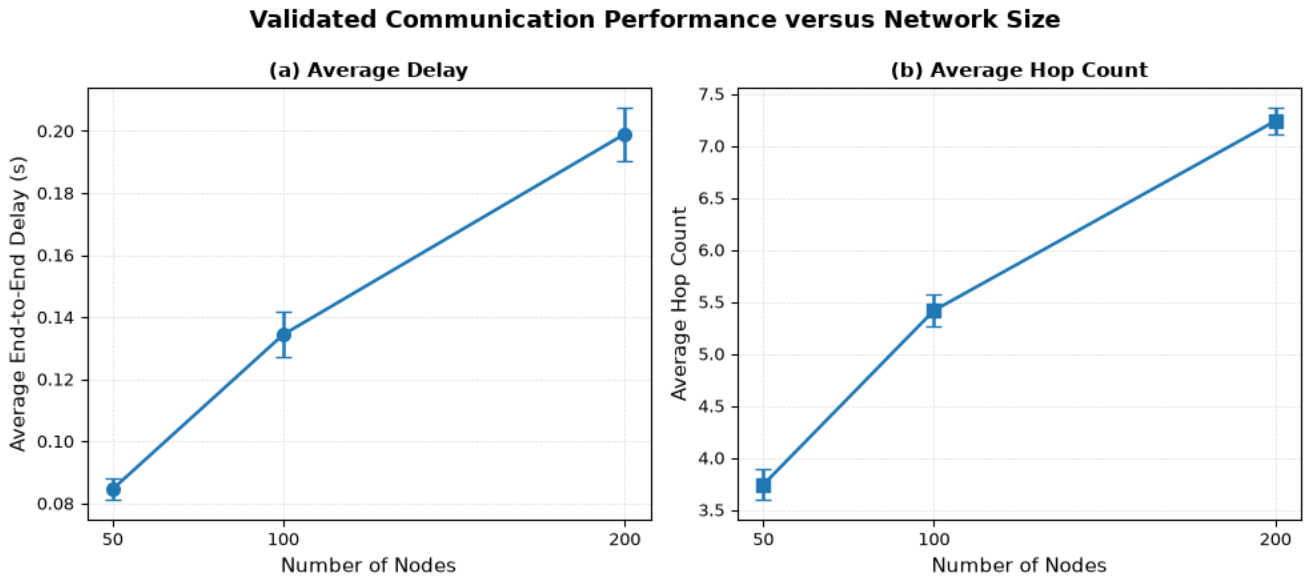


Figure 5. Validated average end-to-end delay and hop count with standard deviation across different network sizes.

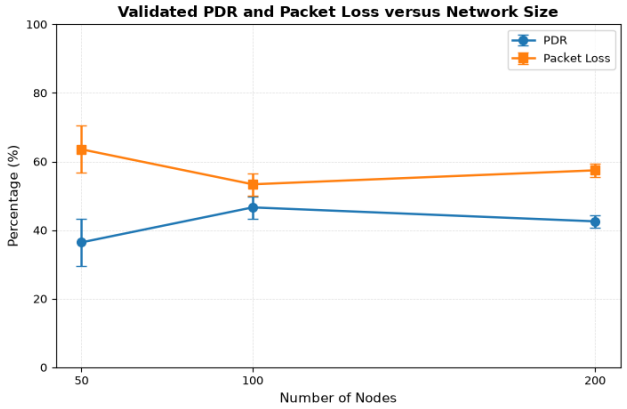


Figure 6. Validated packet delivery ratio and packet loss across different network sizes. Error bars represent standard deviation across five independent seeds.

lay. A configuration that reduces activity may save energy but can reduce the availability of forwarding opportunities. Conversely, maintaining greater communication activity can support packet delivery while increasing energy expenditure. The Pareto formulation is therefore useful because it exposes these competing operating points rather than hiding them behind a single weighted objective.

5.4 Robustness Across Random Seeds

The selected configurations were evaluated using five independent random seeds to determine whether the observed behavior persists across different stochastic realizations. The results show measurable variation in all principal metrics, particularly PDR.

For the 50-node configuration, the PDR standard deviation is 6.8676 percentage points, compared with 3.2558 percentage points for 100 nodes and 1.8428 percentage points for 200 nodes. Thus, the 50-node configuration exhibits greater seed-to-seed variation in delivery performance.

Energy and delay show comparatively smaller absolute variations. The energy standard deviations are 0.4275 J, 1.0215 J, and 2.1288 J, while the delay standard deviations are 0.00347 s, 0.00737 s, and 0.00851 s for 50, 100, and 200 nodes, respectively. These observations demonstrate why multi-seed validation is important. A single simulation realization could give an incomplete picture of the behavior of an optimized configuration. Repeating the evaluation with independent seeds provides a more informative assessment of the stability of the selected solution.

5.5 Implications for Dense IoT Networks

The density-wise results have a practical implication for dense IoT deployments. Increasing the number of nodes alone should not be regarded as a guaranteed mechanism for improving network reliability. Additional nodes can increase the available communication opportunities, but they can also increase forwarding activity, communication overhead, and path length.

The proposed formulation addresses this issue by allowing node activity and communication decisions to be selected jointly. The resulting Pareto solutions can therefore be interpreted as different operating points for different network conditions rather than as a single universally optimal configuration.

The principal contribution of this analysis is consequently not the use of NSGA-II itself, which is a well-established optimization method [16], but the systematic examination of the joint activity–communication trade-off across network densities and the subsequent multi-seed validation of the selected configurations.

5.6 Limitations

Several limitations should be considered when interpreting the results. First, the present evaluation uses three network sizes and five random seeds; therefore, broader density ranges and additional stochastic realizations could provide stronger evidence about scalability. Second, the current study focuses on the selected Pareto configurations rather than claiming universal optimality for all possible network operating conditions. Third, PDR values observed in the present experiments

are relatively low, so reliability-related conclusions should be interpreted as comparative behavior of the evaluated configurations rather than as evidence that the configurations satisfy an application-specific reliability requirement.

These limitations also identify directions for future work, including larger network populations, additional traffic and topology conditions, stronger reliability constraints, and comparison with independently implemented baseline protocols.

6. CONCLUSION AND FUTURE WORK

This study presented a Pareto-based framework for jointly optimizing node activity and communication decisions in dense IoT sensor networks. The formulation considers total energy consumption, average end-to-end delay, and packet delivery reliability as competing objectives. NSGA-II was employed as the multi-objective optimization engine to obtain non-dominated configurations, while the selected configurations were subsequently evaluated under independent stochastic conditions.

The density-wise evaluation considered networks containing 50, 100, and 200 nodes. The validated results show that increasing network size leads to higher energy consumption and communication delay. Mean energy increased from 8.6090 J for 50 nodes to 70.6780 J for 200 nodes, while mean delay increased from 0.08458 s to 0.19901 s. Average hop count also increased from 3.7421 to 7.2395. These results indicate that increasing network density introduces additional communication and forwarding costs.

Packet delivery reliability exhibited a non-monotonic behavior. The highest mean PDR among the evaluated configurations was observed for the 100-node network (46.6317%), while the 50-node and 200-node configurations achieved 36.4393% and 42.5616%, respectively. Thus, increasing the number of nodes did not produce a uniform improvement in packet delivery performance.

The selected chromosomes retained heterogeneous node activity, with duty-cycle values bounded between 0.2 and 0.8. This supports the use of node-specific activity decisions rather than a single homogeneous duty-cycle value. The corresponding routing-λ values also varied across network sizes, reinforcing the role of joint activity and communication decisions in determining the resulting operating point.

A five-seed validation procedure was used to examine the robustness of the selected configurations. The use of independent seeds revealed measurable stochastic variation, particularly in PDR, while the mean energy and delay trends remained consistent across the evaluated network sizes. This validation provides stronger evidence than relying on a single simulation realization.

The main contribution of the study is therefore the systematic analysis of the energy–delay–reliability trade-off produced by jointly controlling node activity and communication decisions under increasing network density. The work does not treat NSGA-II as the novelty; instead, NSGA-II provides the optimization mechanism through which the proposed decision representation and Pareto trade-offs are explored.

6.1 Future Work

Future investigations can extend the framework in several directions. Larger network sizes and a broader range of densities can be evaluated to establish more comprehensive scalability trends. Additional traffic patterns and topology conditions can also be incorporated to determine whether the observed trade-offs remain stable under different operating environments.

A stronger reliability constraint can be introduced in future experiments so that Pareto solutions are evaluated not only according to their relative trade-offs but also against application-specific PDR requirements. Further baseline experiments can provide controlled comparisons between fixed-activity routing, activity-only optimization, routing-only optimization, and the proposed joint optimization.

Finally, the framework can be extended to incorporate additional network objectives and constraints, such as network lifetime, residual-energy balance, congestion, and fault tolerance. These extensions would allow the proposed activity–communication formulation to be evaluated under more demanding dense-IoT scenarios.

REFERENCES

[1] I. F. Akyildiz, W. Su, Y. Sankarasubramaniam, and E. Cayirci, "Wireless sensor networks: A survey," *Computer Networks*, vol. 38, no. 4, pp. 393–422, 2002.

[2] S. A. Abbas, L. Farzinvash, and M. Zolfy, "A two-phase genetic algorithm approach for sleep scheduling, routing, and clustering in heterogeneous wireless sensor networks," *Network*, vol. 5, no. 4, p. 50, 2025.

[3] M. K. Roberts, S. Jeevanandham, J. Lloret, and F. Dahan, "An innovative dual-phased synergistic energy management approach for WSNs using enhanced sleep/awake scheduling and adaptive routing process," *Simulation Modelling Practice and Theory*, vol. 142, p. 103120, 2025.

[4] W. R. Heinzelman, A. P. Chandrakasan, and H. Balakrishnan, "Energy-efficient communication protocol for wireless microsensor networks," in *Proceedings of the 33rd Hawaii International Conference on System Sciences*, 2000, pp. 1–10.

[5] M. A. Tawfeek, I. Alrashdi, M. Alruwaili, L. Jamel, G. F. Elhady *et al.*, "Improving energy efficiency and routing reliability in wireless sensor networks using modified ant colony optimization," *EURASIP Journal on Wireless Communications and Networking*, vol. 2025, p. 22, 2025.

[6] A. A. Lata, M. Kang, and S. Shin, "FCM-OR: A local density-aware opportunistic routing protocol for energy-efficient wireless sensor networks," *Electronics*, vol. 14, no. 9, p. 1841, 2025.

[7] C. Rao, M. Kan, P. Zhou *et al.*, "A novel multi-objective energy-efficient clustering optimization scheme based on heuristic intelligence for wireless sensor networks," *Scientific Reports*, vol. 15, p. 36988, 2025.

[8] Y. Zhang, L. Yang, and Y. Tan, "Energy-efficient adaptive routing in heterogeneous wireless sensor networks via hybrid PSO and dynamic clustering," *Journal of Cloud Computing*, vol. 14, p. 46, 2025.

[9] M. J. Kavitha, M. R. Geetha, and R. I. Sajan, "Knowledge-based adaptive routing for energy efficiency and attack detection in ad hoc wireless sensor networks," *Computer Networks*, vol. 259, p. 111086, 2025.

[10] I. Samoylenko, V. Fedorenko, and V. Samoylenko, "Adaptive data relay transmission in wireless sensor networks for reliable crop growth monitoring," *Computers and Electronics in Agriculture*, vol. 234, p. 110367, 2025.

[11] B. Rana, Y. Singh, P. K. Singh, K. Z. Ghafoor, and S. Shrestha, "A hybrid approach for energy-efficient routing in IoT using duty cycling and improved ant colony," *IET Communications*, vol. 19, no. 1, pp. 1–19, 2025.

[12] S. Thakur, N. I. Sarkar, and S. Yongchareon, "AI-driven energy-efficient routing in IoT-based wireless sensor networks: A comprehensive review," *Sensors*, vol. 25, no. 24, p. 7408, 2025.

[13] W. Zeng, Z. Wang, S. Yang, D. He, and S. Chan, "ICMH-CHR: An intra-cluster multi-hop based cluster head rotation protocol for wireless sensor networks," *Ad Hoc Networks*, vol. 174, p. 103829, 2025.

[14] L. Yang, D. Zhang, L. Li, and Q. He, "Energy efficient cluster-based routing protocol for WSN using multi-strategy fusion snake optimizer and minimum spanning tree," *Scientific Reports*, vol. 14, no. 1, p. 16786, 2024.

[15] Z. Wang, Y. Yang, X. Luo, D. He, and S. Chan, "Energy-efficient clustering and routing for wireless sensor networks by applying a spider wasp optimizer," *Ad Hoc Networks*, vol. 174, p. 103841, 2025.

[16] K. Deb, A. Pratap, S. Agarwal, and T. Meyarivan, "A fast and elitist multiobjective genetic algorithm: NSGA-II," *IEEE Transactions on Evolutionary Computation*, vol. 6, no. 2, pp. 182–197, 2002.